Chemosphere 359 (2024) 142278

Contents lists available at ScienceDirect

Chemosphere

journal homepage: www.elsevier.com/locate/chemosphere

The stunting effect of an oxylipins-containing macroalgae extract on sea urchin reproduction and neuroblastoma cells viability

Chiara Martino [a,b,*,1], Rosario Badalamenti [a,1], Monica Frinchi [c,**,1], Roberto Chiarelli [a], Antonio Palumbo Piccionello [a], Giulia Urone [c], Manuela Mauro [a], Vincenzo Arizza [a,b], Claudio Luparello [a,b], Valentina Di Liberto [c], Giuseppa Mudò [c], Mirella Vazzana [a,b]

[a] Department of Biological, Chemical and Pharmaceutical Sciences and Technologies (STEBICEF), University of Palermo, Via Archirafi 18, 90123, Palermo, Italy
[b] NBFC, National Biodiversity Future Center, Piazza Marina 61, 90133, Palermo, Italy
[c] Department of Biomedicine, Neurosciences and Advanced Diagnostics, University of Palermo, Corso Tukory 129, 90134, Palermo, Italy

HIGHLIGHTS

- Seven oxylipins were identified in extract of seaweed *Ericaria brachycarpa* (EBE).
- Stage-specific EBE effect was found in developing *Arbacia lixula* sea urchin embryos.
- EBE was toxic for neuroblastoma cells and not for the differentiated counterpart.
- Autophagy and apoptosis were induced by EBE in embryos and neuroblastoma cells.
- Expression levels of heat shock proteins were modulated by EBE in embryos and cells.

GRAPHICAL ABSTRACT

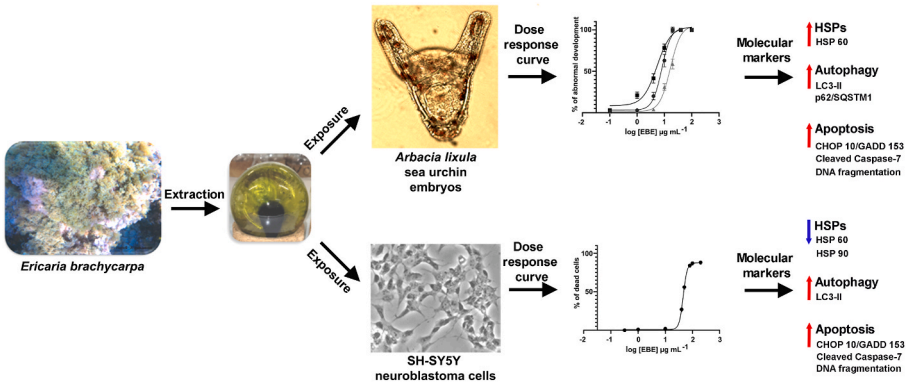

ARTICLE INFO

Handling editor: Maria Augustyniak

Keywords:
Marine drugs
Ecotoxicology
Oxylipins
Developmental abnormality
SH-SY5Y
Apoptosis

ABSTRACT

Different bioactive molecules extracted from macroalgae, including oxylipins, showed interesting potentials in different applications, from healthcare to biomaterial manufacturing and environmental remediation. Thus far, no studies reported the effects of oxylipins-containing macroalgae extracts on embryo development of marine invertebrates and on neuroblastoma cancer cells. Here, the effects of an oxylipins-containing extract from *Ericaria brachycarpa,* a canopy-forming brown algae, were investigated on the development of *Arbacia lixula* sea urchin embryos and on SH-SY5Y neuroblastoma cells viability. Embryos and cells were exposed to concentrations covering a full 0–100% dose-response curve, with doses ranging from 0 to 40 μg mL^{-1} for embryos and from 0 to 200 μg mL^{-1} for cells. These natural marine toxins caused a dose-dependent decrease of normal embryos development and of neuroblastoma cells viability. Toxicity was higher for exposures starting from the gastrula

* Corresponding author. Department of Biological, Chemical and Pharmaceutical Sciences and Technologies (STEBICEF), University of Palermo, Via Archirafi 18, 90123, Palermo, Italy.
** Corresponding author.
E-mail addresses: chiara.martino@unipa.it (C. Martino), monica.frinchi@unipa.it (M. Frinchi).
[1] These authors equally contributed to the work.

https://doi.org/10.1016/j.chemosphere.2024.142278
Received 22 March 2024; Received in revised form 3 May 2024; Accepted 5 May 2024
Available online 9 May 2024

embryonal stage if compared to the zygote and pluteus stages, with an EC_{50} significantly lower by 33 and 68%, respectively. Embryos exposed to low doses showed a general delay in development with a decrease in the ability to calcify, while higher doses caused 100% block of embryo growth. Exposure of SH-SY5Y neuroblastoma cells to 40 μg mL^{-1} for 72 h caused 78% mortality, while no effect was observed on their neuronal-like cells derivatives, suggesting a selective targeting of proliferating cells. Western Blot experiments on both model systems displayed the modulation of different molecular markers (HSP60, HSP90, LC3, p62, CHOP and cleaved caspase-7), showing altered stress response and enhanced autophagy and apoptosis, confirmed by increased fragmented DNA in apoptotic nuclei. Our study gives new insights into the molecular strategies that marine invertebrates use when responding to their environmental natural toxins and suggests the *E. brachycarpa*'s extract as a potential source for the development of innovative, environmentally friendly products with larvicide and antineoplastic activity.

Abbreviations

MFSW	millipore filtered seawater
EBE	*Ericaria brachycarpa* extract
HEPEs	hydroxyacids
hpf	hours post fertilization
MTT	3-(4,5-dimethylthiazol 2-yl)-2,5-diphenyltetrazolium bromide
HSPs	heat shock proteins
TUNEL	TdT-mediated dUTP nick-end labeling
WB	western blot
EC50	half maximal effective concentration
NOEC	no observed effect concentration

1. Introduction

Extracts and molecules obtained from several marine species have shown anticancer, anti-angiogenic, anti-inflammatory and wound healing/skin regeneration abilities, finding applications in healthcare, biomaterial manufacturing and environmental remediation (Conte et al., 2020; Pereira and Cotas, 2023; Librizzi et al., 2023). Among marine organisms, macroalgae are sessile organisms that need to constantly adapt to either the abiotic and biotic components of the marine ecosystem and developed competitive and complex adaptations to safeguard their species, including the production of a wealth of bioactive molecules via their secondary metabolism as a chemical strategy against environmental stressors and against their predators (Budzałek et al., 2021; Seth et al., 2024). Driven by the increased global interest in natural products, macroalgae are currently being investigated as a primary source of new classes of molecules with greater bioavailability and efficacy and less toxicity, for nutraceuticals and pharmaceutical applications (Adarshan et al., 2023). Since therapeutic resistance is one of the main causes for concern in oncology, several algal-extracted compounds have been characterized and their anticarcinogenic activity was demonstrated *in vivo* and *in vitro* (Thaman et al., 2023). Neuroblastoma represents the most common extracranial solid pediatric cancer and is sadly one of the leading causes of cancer-related deaths among children since most patients develop drug resistance, thus highlighting the need for testing new molecules for its treatment (Dhamdhere and Spiegelman, 2024). Moreover, extracts and molecules obtained from macroalgae have been tested on invertebrates, showing a wide range of activities, including feeding-deterrent abilities against sea urchins grazing (Budzałek et al., 2021).

Among secondary metabolites, oxylipins are generated from polyunsaturated fatty acids via the lipoxygenase pathway, accumulating as a reaction to abiotic and biotic stressors (Barbosa et al., 2016). Diatoms-derived oxylipins are produced after cell damage and during grazing by predators (Ruocco et al., 2019), and their release in the marine environment can subsequently induce reproductive impairment and teratogenic effects on their predators, including copepods and sea urchins (Ruocco et al., 2019; Lauritano and Ianora, 2020). Exposure of *Paracentrotus lividus* embryos to diatoms-derived polyunsaturated aldehydes in the μM range showed a dose-dependent block of the first cleavage and an increase in the percentage of malformed and delayed embryos, together with a large amount of fragmented DNA (Romano et al., 2010). Other diatoms-derived oxylipins, hydroxyacids (HEPEs), had low toxicity to adult copepods but highly impaired their gametes and nauplii (Fontana et al., 2007) and caused a dose-dependent effect with the induction of skeletal malformations in *P. lividus* embryos (Varrella et al., 2016). Moreover, diatom-derived oxylipins can induce cell death in different human cancer cell lines in the μM to low mM range (Miralto et al., 1999; Sansone et al., 2014; Ávila-Román et al., 2016). In macroalgae, oxylipins operate in systemic defense mechanisms and are induced responding to different stresses and against grazers and pathogens (Jacquemoud and Pohnert, 2015; Barbosa et al., 2016). While many studies are available on the effect of diatoms-derived oxylipins on marine invertebrates' reproduction and on human cancer cell viability, the biological effect of macroalgae-derived oxylipins is still poorly elucidated.

Among macroalgae, *Ericaria* spp. are canopy-forming brown algae belonging to the Sargassaceae family that live in the Mediterranean rocky coastline. One of these species, *Ericaria brachycarpa* ((J. Agardh) Molinari-Novoa and Guiry, 2020), contribute to form the habitat for the sympatric sea urchins species *P. lividus* and *Arbacia lixula* (Echinodermata: Echinoidea; Bonaviri et al., 2011). The grazing activity of *A. lixula* exerts a primary control on the composition and abundance of canopy-forming macroalgal assemblages, thanks to its strong Aristotle's lantern that allows the scraping of the substrate (Privitera et al., 2008; Bonaviri et al., 2011), causing the formation of barren grounds (Bonaviri et al., 2011; Lawrence, 2013). Numerous molecules have been identified from various species of the *Ericaria* genus, including terpenoids, steroids, phlorotannins and phenolic compounds, some of which showing antimicrobial, cytotoxic and antitumoral features (Amico, 1995; de Sousa et al., 2017).

Here, for the first time, we identified seven oxylipins in the extract of a species of the *Ericaria* genus (*E. brachycarpa*) and tested the effects of this extract on *A. lixula* sea urchin embryos and on the human neuroblastoma SH-SY5Y cell line and their neuronal-like cells derivatives. In order to understand the molecular mechanisms activated in *A. lixula* embryos and SH-SY5Y cells after exposure, we analyzed the expression levels of different proteins involved in the stress response (HSPs) and of molecular markers of the autophagic (LC3 and p62/SQSTM1) and apoptotic (cleaved caspase-7 and CHOP-10/GADD153) pathways. Finally, we evaluated the presence of fragmented DNA through TUNEL staining. To our knowledge, this is the first time that an oxylipin-containing extract from a macroalgae shows growth-restraining activity against embryos of a marine Invertebrate and against neuroblastoma cancer cells.

2. Materials and methods

2.1. E. brachycarpa sampling, extraction and HPLC/MS analysis

The sporophytes of *E. brachycarpa* and adult *A. lixula* sea urchins

were sampled at the littoral of Palermo, in the Northern Sicilian coast, where they naturally coexist, from March to June 2023, as the main reproductive peak for these two species coincide in these months (Hoffmann et al., 1992; Wangensteen et al., 2013). The sporophytes were washed and rinsed to remove debris and epiphytes, then dried at 40 °C in an oven for 48 h. The dried thalli were subsequently finely ground to obtain a powder using a stainless-steel grinder. Metabolites extraction was performed by treating 1 g of the obtained powder with 20 mL of $CHCl_3$/MeOH (2:1 v/v). HPLC/MS analysis of the *Ericaria brachycarpa* extract (EBE) was performed as previously described (Faddetta et al., 2023). Mass spectrum data were analyzed for metabolites annotation using MassHunter Qualitative Analysis B.06.00 and the Metabolomic Workbench database [https://www.metabolomicsworkbench.org/search/ms.php]. Before use, a mother solution of EBE diluted 100 mg/mL in DMSO was prepared and then stored at – 20 °C.

2.2. *A. lixula* sampling, fertilization and exposure

Adult *A. lixula* sea urchins were collected monthly in shallow rocky reefs (2– 8 m), from March to June 2023, during their main reproductive peak (Wangensteen et al., 2013). All animal experiments were carried out following the ARRIVE guidelines in accordance with the U.K. Animals (Scientific Procedures) Act, 1986 and the EU Directive 2010/63/EU for animal experiments. For each experiment, 10 adult-sized sea urchins (weight 41.1 ± 6.4 g) were brought to the tanks in laboratory and fertilized within 24 h of collection. Gametes were collected from at least 3 males and 3 females and examined under the microscope to select quality gametes later used for fertilization, as previously described (Martino et al., 2021). Seawater was collected in the same area and filtered (0.22 μm Millipore filtered seawater, hereafter MFSW). Ten minutes after fertilization, the fertilization success (>95%) was inspected by microscopic examination. After three rinsing in MFSW, 20 mL of fertilized eggs (4000 eggs/mL) were places in 20 mm Petri dishes and exposed to different concentrations of EBE (1, 4, 10, 20 and 40 μg mL^{-1}, hereafter EBE 1, EBE 4, EBE 10, EBE 20 and EBE 40), obtained by dilution of the 100 μg mL^{-1} mother solution in MFSW, with 3 replicate dishes per treatment. A schematic drawing of the experimental design is depicted in Fig. 1A. Embryos were reared at 18 °C, with three developmental endpoints for each treatment: 24 h (G, gastrulae), 48 h (ePl, early plutei) and 72 h (lPl, late plutei, see Fig. 1A). Black rods in lines 1, 3 and 6 represent control treatments at 24, 48 and 72 h (Fig. 1A). Grey rods in lines 2, 4 and 7 represent the treatments for 24, 48 and 72 h with different concentrations of EBE added at 0 h post fertilization (hpf, hereafter 0 hpf EBE 1/4/10/20/40, Fig. 1A). Lines 5 and 8 represent treatments with EBE added at 24 and 48 hpf, respectively (hereafter 24 hpf EBE 1/4/10/20/40 and 48 hpf EBE 1/4/10/20/40) (see Fig. 1A). Line 9 represents the recovery experiment, with embryos reared for 24 h in the EBE 40 treatment and then cultivated in MFSW till the 72 h endpoint (Fig. 1A). To determine whether DMSO influenced development, control embryos were exposed to the sole vector and the effect on development evaluated.

2.3. Sea urchin embryos morphological and morphometrical analysis

Every 24 h, 100 embryos were sampled, examined microscopically (Leica DCF420C), photographed using a digital camera and scored for normal/abnormal development. A total of 100 embryos per each replicate dish per each fertilization experiment were scored. Since controls and embryos exposed to the lowest doses of EBE (EBE 1 and 4) reached the gastrula stage at 24 h and the four-armed pre-feeding echinopluteus stage at 48–72 h, using ImageJ (ver 1.46 r) we measured the changes of three morphological parameters to compare the ability to correctly grow and calcify: the full diameter at 24 h, the length of the post-oral arm (PO), and larval body width (BW) at 48 and 72 h (Fig. 1B, $n = 11$). Post-oral arm length represents a well-known metric of echinopluteal growth and calcification and BW was used to analyze changes in larval shape in response to EBE exposure (Byrne et al., 2013; Martino et al., 2021; Wangensteen et al., 2013). It was not possible to obtain these morphometric measures at the higher doses (EBE 10, 20 and 40) because embryos presented major developmental aberrations.

2.4. SH-SY5Y cell culture, differentiation and exposure

Undifferentiated proliferating and differentiated SH-SY5Y cells were cultured as previously described by Nuzzo et al. (2023). To establish the EBE effect on cells viability, undifferentiated and differentiated cells were planted respectively at the density of 20,000 and 14,000 cells/well on 96-well plates in a final volume of 100 μL/well and subsequently exposed to different EBE doses (1, 10, 40, 50, 80, 100, 200 μg mL^{-1}) for 24 h, diluting the mother solution in growth medium. Then, a time course experiment was performed in the EBE 40 treatment at three different time points (24, 48 and 72 h). In all the experiments, control

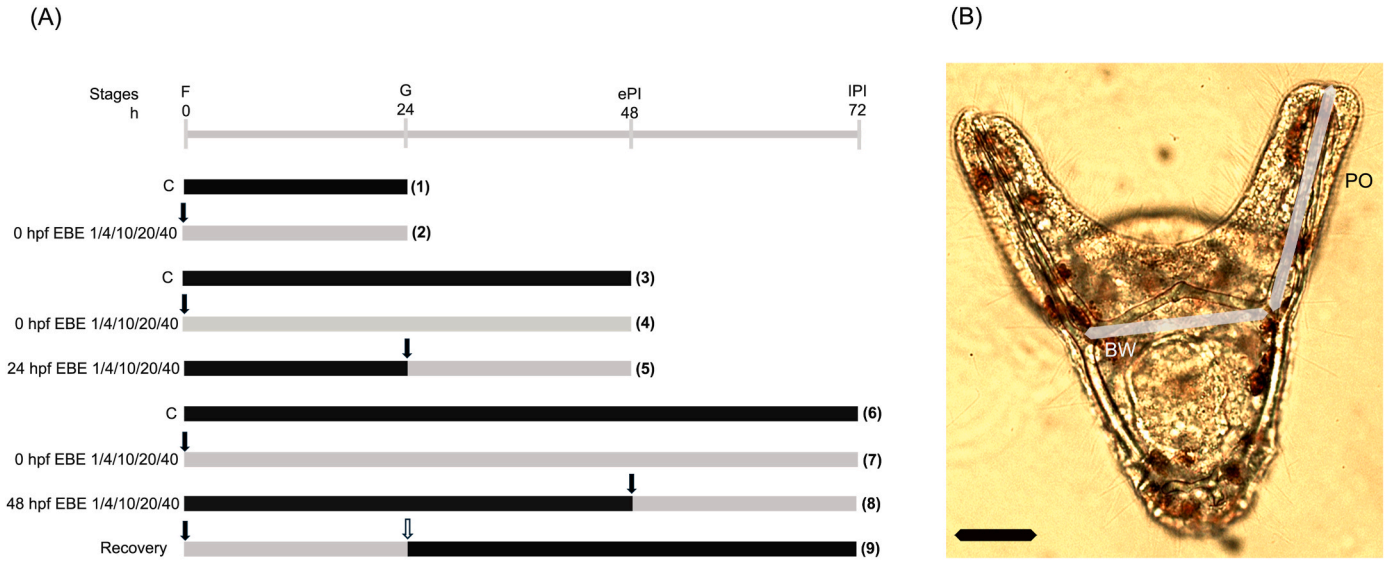

Fig. 1. A) Schematic drawing of the experimental design for *A. lixula* embryos exposure. Black rods, culture in MFSW; grey rods, culture in EBE-containing MFSW. F, fertilization; G, gastrula; ePl, early pluteus; lPl, late pluteus. Black arrows indicate the start of EBE exposure in the different treatments; white arrow indicates the start of recovery in MFSW. B) Morphological traits measured on *A. lixula* plutei: BW, body width; PO, post-oral skeletal rod. Bar: 50 μm.

groups received an equal volume of the solvent only.

2.5. Cell treatment and MTT assay

Cell viability was evaluated after 3 h incubation at 37 °C with 3-(4,5-dimethylthiazol-2-yl)-2,5-diphenyltetrazolium bromide (MTT, 0.5 mg/mL, Sigma-Aldrich), as previously described (Nuzzo et al., 2021). The obtained formazan was dissolved with DMSO and the relative absorbance was read at 570 nm in a Thermo Scientific™ Multiskan™ GO microplate spectrophotometer.

2.6. Dose-response curves

To test whether the sensitivity of *A. lixula* embryos to EBE exposure differed with the developmental stage at which exposures were initiated, we performed three dose–response curves for 24 h treatments starting at 0, 24 and 48 hpf. Also, to test the toxic effects of EBE on neuroblastoma proliferating cells, SH-SY5Y cells were exposed for 24 h at different concentrations. The range of concentrations tested was chosen to cover the full 0–100% curves, with doses ranging from 0 to 40 μg mL^{-1} for embryos and from 0 to 200 μg mL^{-1} for SH-SY5Y cells. The dose-response curves were calculated plotting the percentages of abnormal embryos/dead cells across increasing EBE concentrations fitting a four-parameter logistic function. Two ecotoxicological parameters were determined: EC_{50}, the concentration that gives the half-maximal response, and NOEC, the no observed effect concentration. Based on the EC_{50} and NOEC values, EBE 40 was the dose chosen for subsequent investigations on neuroblastoma cells since it caused a significant reduction of undifferentiated SH-SY5Y cell viability and no effect on differentiated cells. For WB and TUNEL assays on embryos, two doses were chosen, i.e., EBE 4, a sub-lethal concentration below the EC_{50} values, and EBE 40, a cytotoxic concentration causing 100% block of first cleavage. Data were analyzed using GraphPad Prism 9.0.2. software (GraphPad Software, Inc., La Jolla, CA, USA).

2.7. Protein extraction, electrophoretic analysis and protein gel blotting

Protein extraction, electrophoresis, immunoblotting analysis and image acquisition were performed according to Chiarelli et al. (2021) for embryos and to Scordino et al. (2024) for SH-SY5Y cells. The following antibodies were used: HSP 60 (H3524 Sigma-Aldrich) diluted 1:500, HSP 90 (sc-13119 Santa Cruz Biotechnology) diluted 1:1000, Cleaved Caspase-7 (9491 Cell Signaling) diluted 1:1000, LC3 (L8918 Sigma-Aldrich) diluted 1:1000, p62/SQSTM1 (Sigma-Aldrich, P0068) diluted 1:500; CHOP-10/GADD153 (sc-7351 Santa Cruz Biotechnology) diluted 1:300, β-actin (sc-47778 Santa Cruz Biotechnology) diluted 1:10,000. As secondary antibodies, we used the ECLTM anti-rabbit IgG horseradish peroxidase linked whole antibody from donkey (GE Healthcare, NA934) or anti-mouse from sheep (GE Healthcare, NA931) diluted 1:2500 with TBS-T for embryos, and goat anti-rabbit IgG (sc-2004, Santa Cruz Biotechnology) horseradish peroxidase-conjugated diluted 1:8000, anti-mouse IgG (sc-2005 Santa Cruz Biotechnology) diluted 1:6500 or Cy3 anti-rabbit IgG (115-165-003 Jackson ImmunoResearch) diluted 1:5000 for SH-SY5Y cells. In embryos, ponceau S staining was used for total protein normalization, since the levels of housekeeping proteins, including actin, changed during developmental phases and under different experimental conditions as many of these proteins, including actin. In SH-SY5Y, β-actin was used for total protein normalization. Data are presented as mean of optical density values ± standard deviation (SD) of triplicate experiments ($n = 3$).

2.8. DNA fragmentation assay

At all the experimental endpoints (see Fig. 1A), 2 mL of the embryo cultures taken from each of the three dishes per treatment were mixed and subsequently fixed with 4% paraformaldehyde for 1 h at room temperature, washed in MFSW and stored until use in pure methanol at -20 °C. SH-SY5Y cells were grown in 12 mm diameter round glass coverslips at the density of $8 \cdot 10^4$. Cells exposed to EBE 40 were collected at three different time points, 24, 48 and 72 h, fixed with 4% paraformaldehyde for 1 h, washed twice with PBS 1X and processed for DNA fragmentation evaluation. DNA fragmentation was analyzed, for both embryo cultures and SH-SY5Y cells, by TUNEL (TdT-mediated dUTP nick-end labelling) assay (Promega) as described by Chiarelli et al. (2021). Positive controls were pre-treated with DNAase before the TdT assay. Negative controls were incubated with nucleotide mix (fluorescein 12-dUTP), without the TdT enzyme. The fragmented labelled chromatin was observed under a 20× objective, using a fluorescence microscopy (Olympus BX50). Quantitative analysis was carried out using ImageJ 1.46r software after acquisition thought a digital camera (Nikon Sight DS-U1).

2.9. Statistical analysis

For sea urchin embryos, statistical analysis was performed as described by Martino et al. (2021), with some modifications. Briefly, since each dish had a different set of embryo genotypes and the experiment was repeated three times resulting in 9 replicate dishes per each treatment, $n = 9$ (Martino et al., 2021). Percentage data for each of the morphological categories, data on PO and BW lengths, WB results and TUNEL assay results were analyzed by two-way analysis of variance (ANOVA), with EBE concentration and the exposure starting time (hpf) as fixed factors. For SH-SY5Y cells, data were collected from three independent experiments, with at least 3 replicates per treatment. For SH-SY5Y cells, controls were considered equal to 1 in WB and to 100% in cell viability assays. Outliers were identified using the Rout method (Q = 5%) and results were analyzed by one-way ANOVA. Tukey's HSD test was used as Post-hoc test for mean comparison and homogeneity of variance was checked and confirmed using Levene's test for embryos and Shapiro–Wilk's test for cells. For data not normally distributed, statistical evaluations were performed by Kruskal–Wallis test, followed by Dunn's multiple comparison test. The analyses were performed using the Statistica 13.2 software (StatSoft, Tulsa, OK, USA) for embryos and GraphPad Prism 9.0.2. software (GraphPad Software, Inc., La Jolla, CA, USA) for cells. $P < 0.05$ was set as the level of significance.

3. Results

3.1. Characterization of the oxylipins in EBE

Considering the potential interest toward oxylipins as agents of reproductive failure and antitumoral compounds (Miralto et al., 1999; Luo et al., 2006; Christensen, 2020), a qualitative analysis of the lipids from EBE was performed by HPLC-MS in negative mode, allowing their characterization. Seven oxygenated lipids were identified (Table 1), among these cyclic derivative oxo-phytodienoic acid 1 and linear hydroxylated fatty acids 2–7 were found, similarly to what previously found in brown algae (Ritter et al., 2008). The carbon lengths of these oxylipins (C16 to C20) are in line with the vast majority of these compounds, derived from lipoxygenases metabolism of polyunsaturated fatty acids precursors found in marine organisms, that display carbon lengths ranging from C16 to C22 (Gerwick and Singh, 2002). Except for compound 1 (Oxo-phytodienoic acid), all the other compounds belong to the HEPEs class of oxylipins. Although oxylipins are known from other macroalgal species (Barbosa et al., 2016), to our knowledge this is the first time they have been extracted from species of the *Ericaria* genus.

3.2. Dose-response curves

3.2.1. Sea urchin embryos

First, we established the general response to different concentrations of EBE in *A. lixula* embryos and checked whether the developmental

Table 1
Oxylipins present in EBE.

	Compound	Molecular formula	ESI- [M-H]- (m/z) (Teor.)	ESI- [M-H]- (m/z) (Exp.)	Rt (min)
1	Oxo-phytodienoic acid	$C_{18}H_{28}O_3$	291.1966	291.1979	20.09
2	Hydroxy-octadecatrienoic acid	$C_{18}H_{30}O_3$	293.2122	293.2140	21.29
3	Hydroxy-eicosapentaenoic acid	$C_{20}H_{30}O_3$	317.2122	317.2138	21.80
4	Hydroxy-eicosatetraenoic acid	$C_{20}H_{32}O_3$	319.2279	319.2294	23.04
5	Hydroxy-eicosapentaenoic acid isomer	$C_{20}H_{30}O_3$	317.2122	317.2136	23.51
6	Hydroxy-palmitic acid	$C_{16}H_{32}O_3$	271.2279	271.2291	25.82
7	Hydroxy-oleic acid	$C_{18}H_{34}O_3$	297.2435	297.2422	26.33

exposure windows influenced EBE toxicity. The levels of normally developed embryos observed in controls were >95% and did not significantly differ with those observed in DMSO treatments. Treatments were performed adding EBE just after fertilization (0 hpf) or at 24 and 48 hpf, thus respectively at the gastrula or pluteus stage, to test whether the sensitivity of embryos to EBE exposure differed with the developmental stage at which exposures were initiated (see Fig. 1A). EBE exposure had a significant dose-dependent effect on the development of *A. lixula* embryos ($F_{17,\ 36} = 581.2$, $p < 0.0001$), as well as the developmental stage at which exposures were initiated ($F_{17,\ 36} = 128.4$, $p < 0.0001$) and their interaction (EBE x hpf: $F_{17,36} = 43.8$; $p < 0.0001$). Exposure from fertilization significantly reduced levels of normally developed larvae in parallel with the increase of the EBE concentration by 19.6, 63, and 100%, respectively for the exposure to EBE 4, 10 and 20. Strikingly, the 24 hpf EBE 1 treatment resulted in 21% abnormal embryos, while this dose had no effect in the 0 and 48 hpf treatments. On the contrary, while for the 0 and 24 hpf treatment there was 100% abnormality at EBE 20, in the 48 hpf EBE 20 treatment there was a reduction in levels of normally developed larvae by 58.8%. The dose-response curves, obtained by plotting the percentages of abnormal development against the concentration used, are shown in Fig. 2A and resulted in an EC_{50} value of 8.0 μg mL^{-1} for the 0 hpf treatment (R squared = 0.9948), 5.3 μg mL^{-1} for the 24 hpf treatment (R squared = 0.9868) and 16.4 μg mL^{-1} for the 48 hpf treatment (R squared = 0.9903), while the NOEC values were respectively 0.5, 0.08 and 0.7 μg mL^{-1}. Thus, toxicity was higher in the 24 hpf treatment if compared to the 0 and 48 hpf ones, with an EC50 significantly lower by 33 and 68%, respectively.

3.2.2. SH-SY5Y cells

In order to establish the EBE effects on SH-SY5Y cell viability, we performed an MTT cell sensitivity assay, finding that 24 h EBE exposure produced a dose-dependent effect on undifferentiated SH-SY5Y cell viability ($F_{7,\ 99} = 147.4$, $p < 0.0001$, Fig. 2B). No toxic effects on SH-SY5Y cells was observed at concentrations up to EBE 10, while a decrease of cell viability was observed above this dose. The dose-response curve showed an EC_{50} value of 45.7 μg mL^{-1} (R squared = 0.9998) and a NOEC value of 14.4 μg mL^{-1}. No toxic effects were detected for doses lower than EBE 10, while maximum percentage of cell death was observed starting from EBE 80. EBE 40 was chosen for the next investigations. At this concentration, EBE exposure produced a significant time-dependent reduction in undifferentiated SH-SY5Y cell viability (Fig. 2C), with 78% of dead cells at 72 h, while no significant toxicity was observed in differentiated SH-SY5Y (Fig. 2D), non-proliferating cells with functional and morphological characteristics similar to neurons. Taken together, these data showed that concentrations up to EBE 40 had a specific toxic effect on undifferentiated SH-

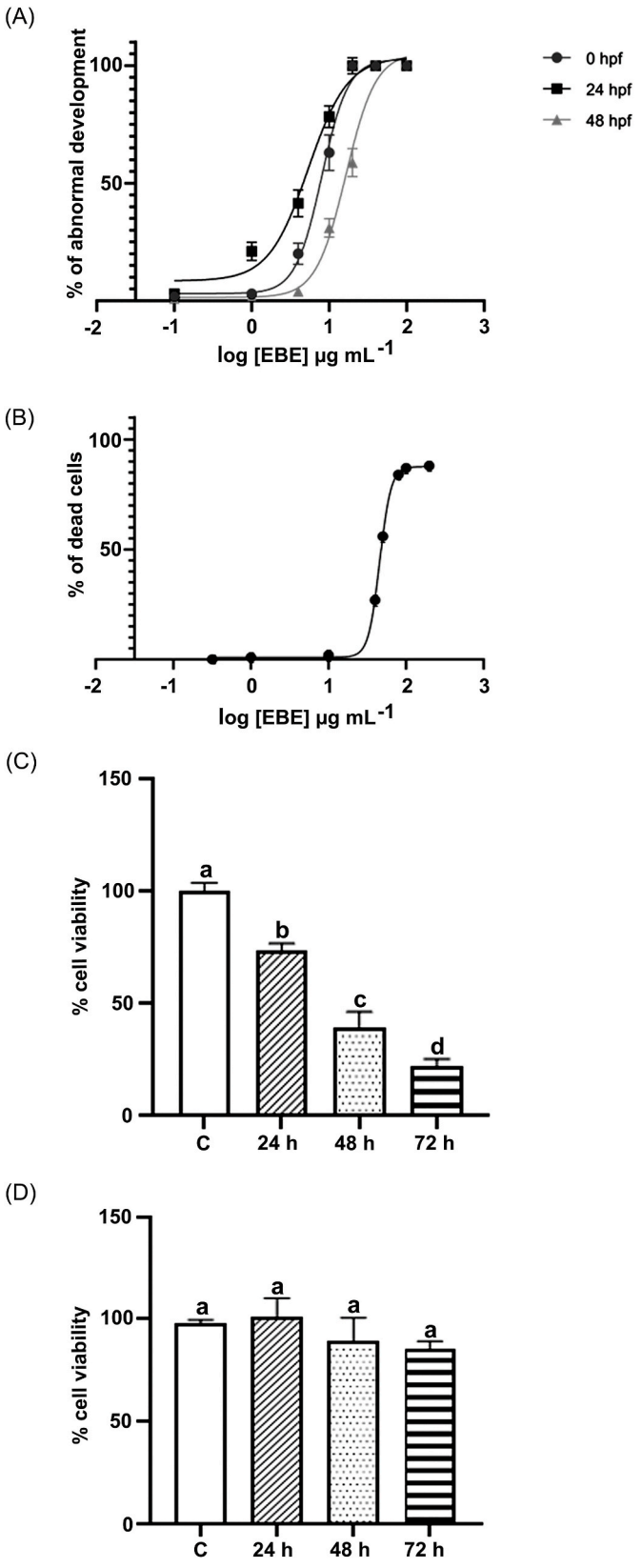

Fig. 2. Dose-response curves across increasing EBE concentrations for percentages of: A) abnormal embryos exposed to EBE from 0, 24 and 48 hpf; B) dead undifferentiated SH-SY5Y cells. Time–course analysis of cell viability following EBE 40 exposure for 24, 48 and 72 h in: C) undifferentiated SH-SY5Y cells and D) differentiated SH-SY5Y cells. Treatments with the same letter do not differ (Tukey HSD). Error bars in Fig. 2B are not visible as ≤ 0.2.

SY5Y cells but not on their neuronal-like cells derivatives, suggesting a preferential selectivity for proliferating cells.

3.3. Morphological analysis of embryos exposed to EBE

3.3.1. Larval morphometry at low doses

EBE exposure from fertilization at the two concentrations below the EC_{50} values (EBE 1 and 4) had no effect until gastrulation (24 h), as both controls and exposed embryos reached all the gastrula milestones with the correct timing, including biomineral deposition (Fig. 3A). The diameter of gastrulae was not significantly different between controls and EBE exposed embryos (not shown). At 48 and 72 h, controls were plutei showing a complex skeletal structure (Fig. 3B, C). Since most embryos exposed to low doses showed delayed development with a decrease in size (Fig. 3D), it was possible to measure their larval size, measured as post-oral rod lengths (PO) and body width (BW), to compare the ability of exposed larvae *vs* controls to correctly grow and calcify (see Fig. 1B).

In control larvae, while the post-oral (PO) rod showed a physiological 25% increase in length from 178.6 ± 12.8 μm at 48 h to 221.9 ± 20 μm at 72 h, no difference was observed in BW, showing that the growth in the plutei size during development is mainly due to increased length and not in width, eventually resulting in a slenderer larval shape (Figs. 3B, C and 4).

At 48 h, exposure to EBE significantly affected both PO arm length ($F_{5,\ 60} = 193.1$, $p < 0.0005$) and larval body width (BW, $F_{5,60} = 28.2$; $p < 0.0005$), as well as the developmental stage at which exposures were initiated (PO: $F_{5,\ 60} = 165$, $p < 0.0005$; BW: $F_{5,\ 60} = 12$, $p < 0.005$) and their interaction (PO: $F_{5,\ 60} = 42.5$, $p < 0.0005$; BW: $F_{5,\ 60} = 14.75$, $p < 0.0005$). Larvae exposed from fertilization to EBE 1 and 4 had respectively 15% (153.9 ± 30.6 μm) and 36% (116.7 ± 30.4 μm) shorter PO rods at 48 h, if compared to controls (Fig. 4A). Strikingly, the maximum reduction in PO length was observed in the 24 hpf treatments at 48 h, with a 68% reduction in PO arm length in the EBE 1 treatment (58.1 ± 5.5 μm) and an 87% reduction in the EBE 4 treatment (23.9 ± 7.08 μm) if compared to 48 h controls (Tukey's HSD PO 48 h: 24 hpf EBE 4 < 24 hpf EBE 1 < EBE 4 < EBE 1 < C, see Figs. 3D and 4A). BW had a significant 17% reduction in the EBE 4 treatment at 48 h (141.6 ± 8.4 μm), but not at EBE 1, if compared to 48 h control plutei (170.4 ± 11.42 μm). Strikingly, in the 24 hpf treatments there was a significant 23% reduction in BW at EBE 1 (138.8 ± 12.9 μm) and a 32% reduction at EBE 4 (122.5 ± 15.1 μm, Tukey's HSD BW 48 h: 24 hpf EBE 4 = 24 hpf EBE 1 = EBE 4 < EBE 1 = C, see Fig. 4A).

At 72 h, EBE exposure had a significant effect both on PO ($F_{5,\ 60} = 45.4$, $p < 0.0001$) and BW ($F_{5,60} = 14.8$; $p < 0.0005$), as well as the developmental stage at which exposures were initiated (PO: $F_{5,\ 60} =$

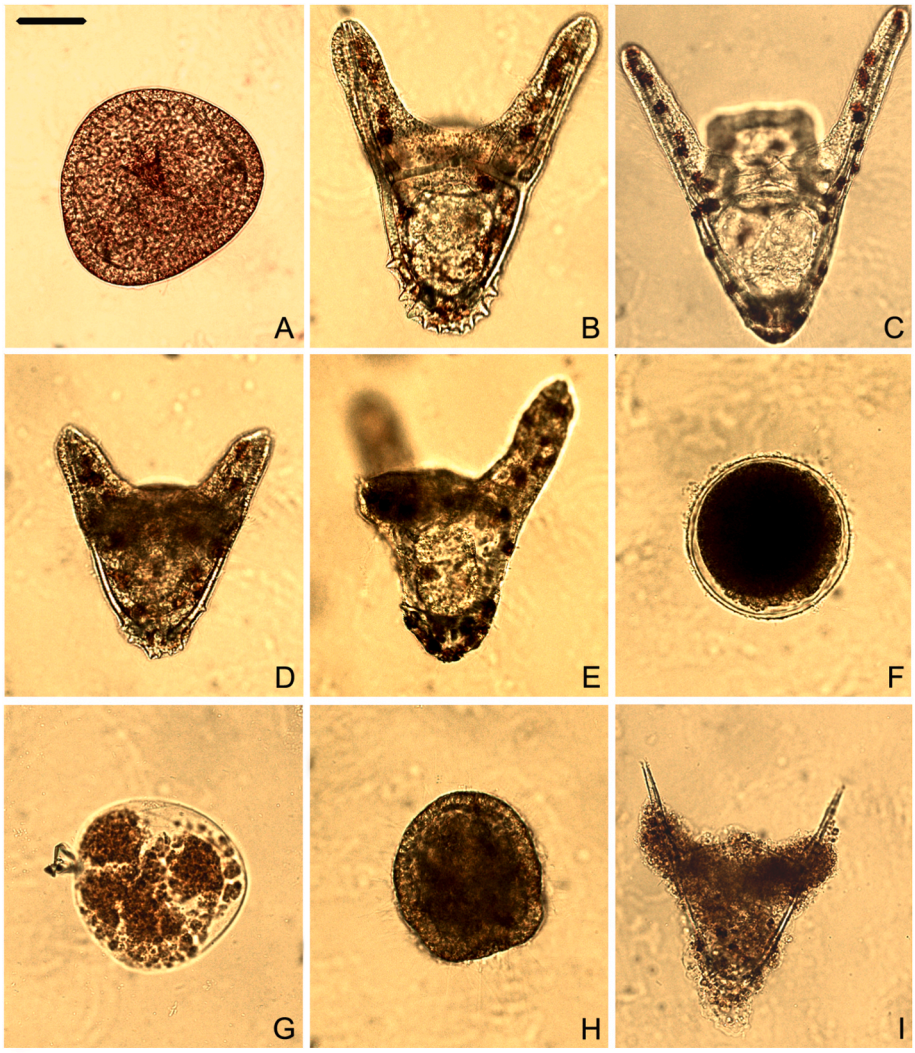

Fig. 3. Morphotypes in control (A–C) and EBE-exposed embryos (D–I). A) control embryo at 24 h; B) control embryo at 48 h; C) control embryo at 72 h; D) delayed embryo at 48 h; E) malformed embryo at 48 h; F) zygote with segmentation inhibition at 24 h; G) apoptotic shrinkage and disassembly into apoptotic bodies at 72 h; H) acute toxicity in the 24 hpf EBE 40 treatment; I) apoptotic cell death in 48 hpf EBE 40 plutei. Bar = 60 μM in A-B, D-H; 75 μM in C, I.

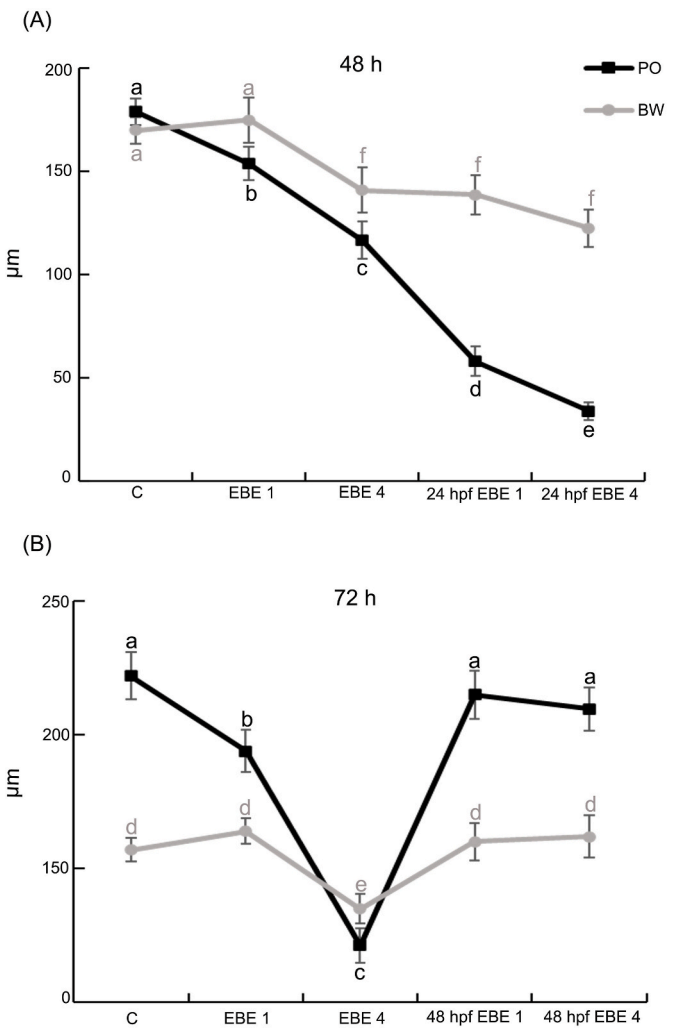

Fig. 4. Larval post-oral arm length and body width measured at 48 (A) and 72 h (B) in response to EBE exposure. Treatments with the same letter do not differ (Tukey HSD).

77.2, $p < 0.0005$; BW: $F_{5, 60} = 4.31$, $p < 0.05$) and their interaction (PO: $F_{5, 60} = 49.5$, $p < 0.0005$; BW: $F_{5, 60} = 14.7$, $p < 0.0005$). Larvae in the 0 hpf EBE 1 and 4 treatments had respectively 13% (193.9 ± 15.7 µm) and 46% (121.2 ± 13.7 µm) shorter PO rods at 72 h, if compared to controls (156.9 ± 8.9 µm) (Fig. 4B, Tukey's HSD PO 72 h: EBE 4 < EBE 1 < C = 48 hpf EBE 1 = 48 hpf EBE 4). For BW, a significant 21% reduction was observed at EBE 4 (135.1 ± 9.4 µm), while no difference was present at EBE 1 (Fig. 4B). Strikingly, no difference was present in the 48 hpf EBE 1 and 4 treatments either for PO or BW (Fig. 4B, Tukey's HSD BW 72 h: EBE 4 < EBE 1 = C = 48 hpf EBE 1 = 48 hpf EBE 4).

3.3.2. Impairment of development at high doses

In the 0 hpf treatment, retarded development and major developmental aberrations were observed at the three concentrations tested above the EC_{50} value (EBE 10, 20 and 40), showing a dose-dependent block of the first cleavage. Only 37% of embryos exposed to EBE 10 normally developed to the pluteus stage at 48 h, while 33% were delayed or abnormal embryos (Fig. 3D, E) and 30% showed cleavage inhibition (Fig. 3F). Treatments with the highest dose (EBE 40) showed 100% block of first cleavage and after 48 h apoptotic shrinkage and disassembly into apoptotic bodies were easily recognized (Fig. 3G).

In the recovery experiment, embryos exposed to EBE 40 for 24 h and then transferred in MSFW for further 48 h showed 100% cleavage inhibition with the first signals of apoptotic cell death, such as convoluted and extension-forming outlines (the phenotype shown in Fig. 3F), demonstrating that once the apoptotic process is initiated after exposure to EBE 40, the cell will be inevitably led to death.

In the 24 and 48 hpf EBE 40 treatments, the progression through developmental stages resulted totally blocked, as gastrulae showed acute toxicity (Fig. 3H) and plutei displayed evident apoptotic features with cells forming extensions and detaching from the skeletal structure (Fig. 3I).

3.4. EBE induces a modulation of heat shock proteins

3.4.1. Sea urchin embryos

Both EBE exposure ($F_{12,26} = 387.8$; $p < 0.0001$) and the developmental stage at which exposures were initiated ($F_{12,26} = 248.2$; $p < 0.0001$) had a significant effect on HSP60 expression, as well as their interaction (EBE x hpf: $F_{12,26} = 108.5$; $p < 0.0001$). While no increase was observed in the EBE 4 treatment, EBE 40 treatments induced the up-regulation of HSP 60 protein levels at 24 h but, strikingly, was not present at 48 and 72 h (Fig. 5A), suggesting the activation of other processes. On the contrary, larvae in the 24 and 48 hpf treatments at both EBE concentrations had significantly ~2-fold higher HSP 60 levels if exposed from the gastrula stage and ~5-fold higher levels if exposed from the pluteus stage, compared to 48 and 72 h controls (Fig. 5A).

3.4.2. SH-SY5Y cells

As shown in Fig. 5B and C, exposure of undifferentiated SH-SY5Y cells for 24 h to EBE 40 treatment induced a significant down regulation of HSP 60 and HSP 90. A significant 24% and 34% reduction in HSP 60 protein levels was respectively observed at 24 h and 48 h, and a further decrease up to 60% was observed at 72 h ($F_{3,36} = 16.09$; $p < 0.0001$). HSP 90 protein levels showed a significant progressive reduction from 43% at 24 h up to 84% at 72 h ($F_{3,36} = 22.38$; $p < 0.0001$).

3.5. EBE modulates the autophagic proteins LC3 and p62/SQSTM1

3.5.1. Sea urchin embryos

The amount of these proteins showed that EBE exposure significantly affected their expression (LC3: $F_{12,26} = 609.3$, $p < 0.0001$; p62: $F_{12,26} = 969.3$, $p < 0.0001$), as well as the exposure starting time (LC3: $F_{12,26} = 246.2$, $p < 0.0001$; p62: $F_{12,26} = 1004.1$, $p < 0.0001$) and their interaction (LC3: $F_{12,26} = 177.6$, $p < 0.0001$; p62: $F_{12,26} = 530$, $p < 0.0001$). The two proteins had similar expression profiles, being down-regulated in the EBE 40 treatments from fertilization (Fig. 6A). In treatments starting at the gastrula and pluteus stages these proteins showed opposite trends, as LC3 was upregulated in the EBE 4 treatments with a ~4-fold increase while p62/SQSTM1 was upregulated in the EBE 40 treatments with a ~12-fold increase at 48 h and a 2.4-fold increase at 72 h (Fig. 6A).

3.5.2. SH-SY5Y cells

The WB analysis showed that EBE 40 treatment induced autophagy in undifferentiated SH-SY5Y cells ($F_{3,36} = 8.578$, $p = 0.0002$), as seen by a significant 2.4-fold increase in LC3 levels following 48 h exposure (Fig. 6B).

3.6. EBE induces a dose-dependent apoptotic-mediated cell death

3.6.1. Cleaved caspase-7 and CHOP-10/GADD153 proteins

3.6.1.1. Sea urchin embryos. Both EBE exposure ($F_{12,26} = 946.9$ $p < 0.0001$) and the hpf treatments ($F_{12,26} = 680.9$; $p < 0.0001$) had a significant effect on caspase-7 expression, as well as their interaction (EBE x hpf: $F_{12,26} = 593.9$; $p < 0.0001$). While only low levels of the protein were present in most treatments, embryos exposed to EBE 40 had a 13-fold increase at 48 h and a 108-fold increase at 72 h, if compared to

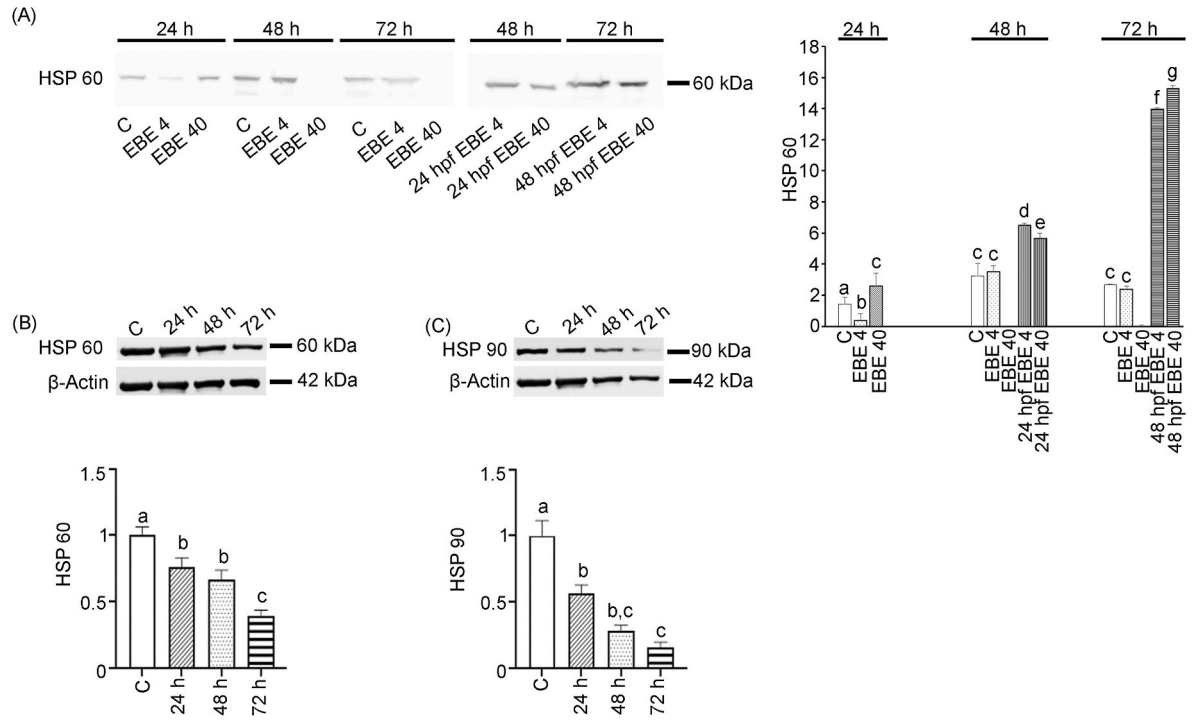

Fig. 5. Western blot analysis of protein levels for: A) HSP 60 in sea urchin embryos; B) HSP 60 and C) HSP 90 after EBE 40 exposure in SH-SY5Y cells. Treatments with the same letter do not differ (Tukey HSD).

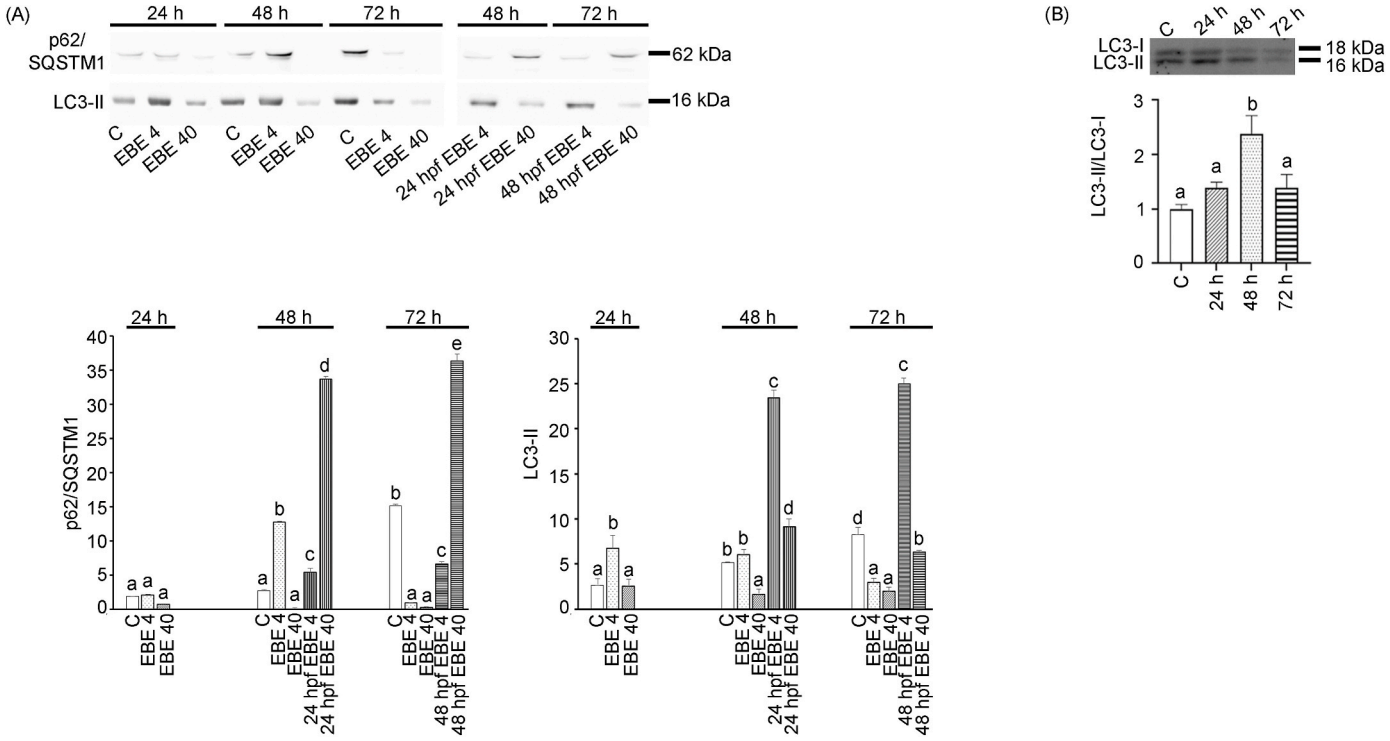

Fig. 6. Western blot analysis of protein levels for: A) p62/SQSTM1 and LC3 in sea urchin embryos; B) LC3 after EBE 40 exposure in SH-SY5Y cells. Treatments with the same letter do not differ (Tukey HSD).

controls (Fig. 7A). Strikingly, also embryos exposed to EBE 40 from the gastrula and pluteus stages had respectively a 57- and a 17-fold increase (Fig. 7A), respectively, demonstrating the massive induction of the execution-phase of cell apoptosis in embryos exposed to the highest dose of EBE.

For CHOP-10/GADD153 expression, WB analysis showed that EBE exposure ($F_{12,26} = 105.5$; $p < 0.0001$) and the developmental stage at which exposures were initiated ($F_{12,26} = 87.5$; $p < 0.0001$) had a significant effect on its protein levels, as well as their interaction (EBE x hpf: $F_{12,26} = 27.2$; $p < 0.0001$). Strikingly, CHOP-10/GADD153 was

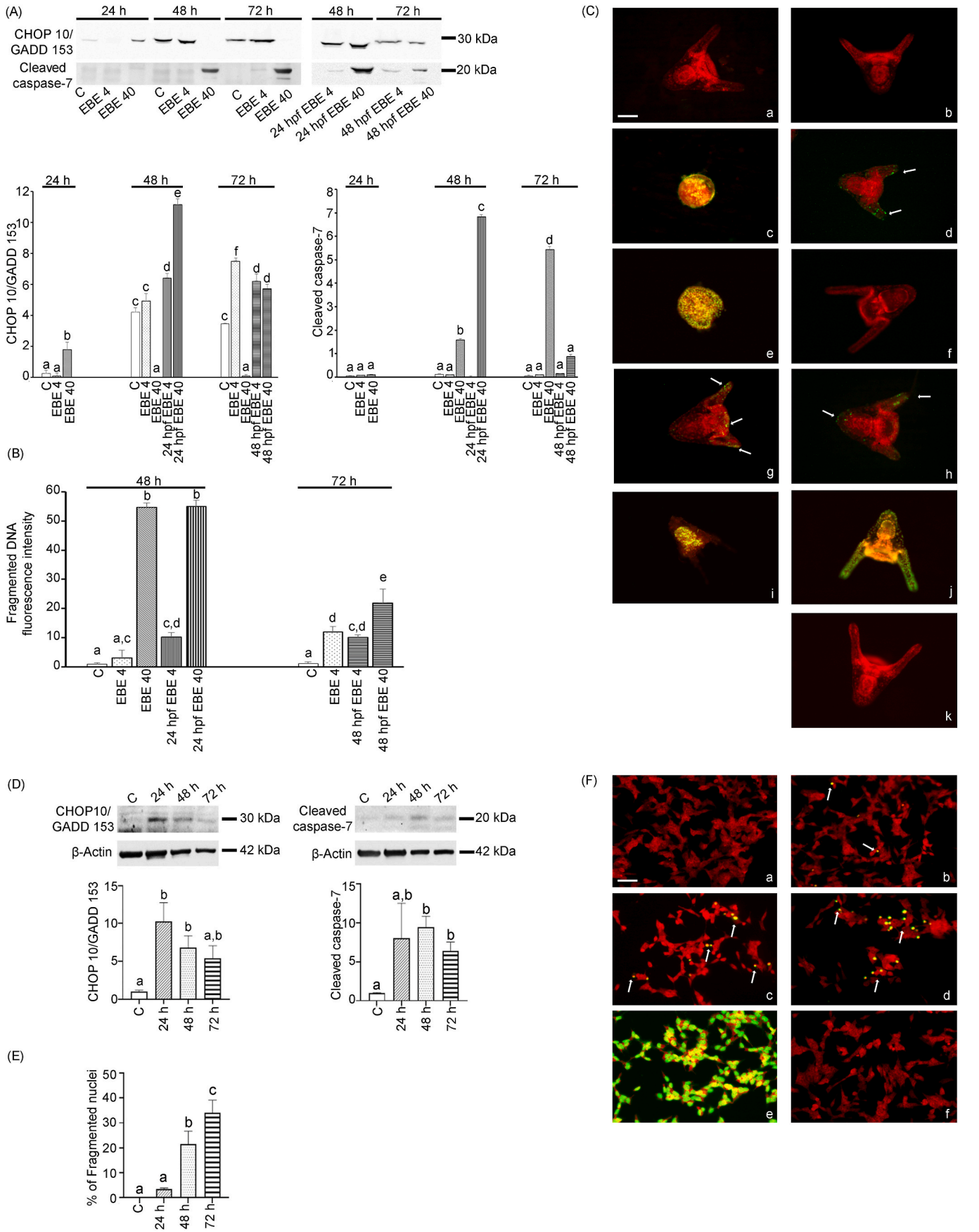

(caption on next page)

Fig. 7. Induction of apoptosis in sea urchin embryos and in SH-SY5Y cells. Western blot analysis of protein levels for CHOP10/GADD153 and Cleaved Caspase-7 in A) sea urchin embryos and D) EBE 40-exposed SH-SY5Y cells. The histograms report the quantification of fluorescence related to fragmented DNA in B) sea urchin embryos and E) SH-SY5Y cells. Treatments with the same letter do not differ (Tukey HSD). Merge of signals from total nuclei stained with propidium iodide and from nuclei with DNA fragmentation (see bright spots indicated by arrows) showing: C) Images of representative embryos at 48 (a–e) and 72 h (f–i) of development. Control embryo at 48 h (a); exposed embryos at 48 h: EBE 4 (b); EBE 40 (c); 24 hpf EBE 4 (d); 24 hpf EBE 40 (e); control embryo at 72 h (f); exposed embryos at 72 h: EBE 4 (g); 48 hpf EBE 4 (h); 48 hpf EBE 40 (i). Positive control embryo (j). Negative control embryo (k). F) Images of SH-SY5Y cells. Control (a) and EBE 40-exposed cells at 24 (b), 48 (c) and 72 h (d). Positive control cells (e). Negative control cells (f). Bar = 60 μm in C) and 45 μm in F).

upregulated in the EBE 40 treatment at 24 h but not present at 48 and 72 h (Fig. 7A), when on the contrary there was a massive expression of caspase-7, likely because the action of CHOP-10/GADD153 in cell cycle arrest is temporally precedent to that of caspase-7. Exposure from the gastrula and pluteus stages also induced higher levels of the CHOP-10/GADD153 protein at both concentrations (Fig. 7A). We also observed a 2-fold increase in the EBE 4 treatment at 72 h if compared to 72 h controls (Fig. 7A).

3.6.1.2. SH-SY5Y cells. Similarly, EBE had a significant effect on CHOP-10/GADD153 expression ($F_{3,34} = 6.734$; $p = 0.0011$) and on caspase-7 expression ($H_{30} = 17.1$; $p = 0.0007$) in undifferentiated SH-SY5Y cells. WB analysis showed very low protein levels of both CHOP-10/GADD153 and cleaved isoform of Caspase-7 in control group (Fig. 7D). Otherwise, a 10-fold increase of CHOP-10/GADD153 was observed in the EBE 40 treatment at 24 h and a significant increase of cleaved isoform of caspase-7 was detected in the EBE 40 treatment at 48 h and 72 h (Fig. 7D).

3.6.2. Chromatin fragmentation

3.6.2.1. Sea urchin embryos. Results of total fragmented apoptotic DNA displayed by TUNEL assay corroborated the WB data about apoptosis. Fig. 7B–C shows equatorial optical sections of representative larvae at 48/72 h and the histogram reporting the amount of apoptotic fragmented DNA. Both EBE exposure ($F_{9,20} = 578$; $p < 0.0001$) and the developmental stage at which exposures were initiated ($F_{9,20} = 93.4$; $p < 0.0001$) had a significant effect on the amount of apoptotic fragmented DNA, as well as their interaction (EBE x hpf: $F_{9,20} = 50.3$; $p < 0.0001$). As previously reported in *P. lividus* larvae, low levels of apoptotic fragmented DNA were present in controls both at 48 and 72 h (Chiarelli et al., 2021; Martino et al., 2021, see Fig. 7B), indicating only basal physiological apoptosis. While no difference was present between controls and larvae in the EBE 4 treatment at 48 h, a significant 10-fold increase was highlighted at 72 h, hallmark of a time-dependent activation of apoptosis (Fig. 7B). No caspase-7 signal was evidenced by WB analysis in the EBE 4 treatment at 72 h since cells were in an advanced stage of apoptosis, where caspase-7 role is already ended but fragmented DNA is still present and visible. Strikingly, the EBE 40 treatment at 48 h determined a 55-fold increase compared to controls, indicating the presence of advanced apoptosis (Fig. 7B). It was not possible to analyze EBE 40 treatment at 72 h by TUNEL because embryos were disassembled into small apoptotic bodies.

Embryos exposed from the gastrula and pluteus stages had a dose-dependent increase of chromatin fragmentation, with a significant 10- and 54- fold increase in the 24 hpf EBE 4 and 40 treatments, and a significant 9.5- and 20.5- fold increase in the 48 hpf EBE 4 and 40 treatments, respectively (Fig. 7B).

Regardless the exposure starting time, embryos exposed to EBE 4 displayed apoptotic nuclei with fragmented DNA only in a restricted group of cells (Fig. 7C), primarily in the apex and PO arms, while embryos exposed to EBE 40 showed massive apoptosis, widespread throughout the embryo (Fig. 6).

3.6.2.2. Chromatin fragmentation in SH-SY5Y cells. EBE exposure ($F_{3,8} = 61$; $p < 0.0001$) led to a significant increase in the amount of apoptotic fragmented DNA in undifferentiated SH-SY5Y cells. As shown in Fig. 7E-F, no signal of fragmented DNA was detected in control cells. Cells exposed to EBE 40 showed a time-dependent response, as the percentage of fragmented nuclei was 3.5, 21 and 34% in cells treated for 24, 48 and 72 h, respectively (Fig. 7E and F).

4. Discussion

Our results provide morphological and molecular evidence of the toxic effects of the oxylipin-containing *E. brachycarpa* extract on *A. lixula* embryos and larvae and on neuroblastoma cells. Oxylipins' diversity in chemical structure and the associated biological effects make them particularly promising for therapeutic strategies, as widely seen for oxylipins derived from plants and microalgae (Blasio and Balzano, 2021; Savchenko et al., 2022), while only few studies exist about the beneficial properties of oxylipins derived from macroalgae (Barbosa et al., 2016). Here, for the first time, we identified seven oxylipins in the extract of a species of the *Ericaria* genus, providing a new insight into the secondary metabolites produced by these brown algae and their potential as therapeutic agents and larvicidal compounds.

Since macroalgae can secrete their secondary metabolites either by direct contact for compounds contained in epidermal glands and secretory trichomes or through masses of water (Gomes et al., 2017), it is likely that sea urchin embryos and larvae may come into direct contact with these molecules. An important finding of this study was that EBE was able to induce a marked delay in development at concentrations below the EC_{50} values, namely EBE 1 and 4. We quantified this delay measuring the decrease of PO and BW lengths and used these values as a proxy of larval calcification (Byrne et al., 2013). Our results showed a major reduction in PO length for larvae exposed from fertilization with respect to controls, posing a threat to larval fitness due to impaired feeding and swimming (Byrne et al., 2013; Martino et al., 2021). Strikingly, the maximum reduction in PO length was observed in the 24 hpf treatments at 48 h, while no difference was present in the 48 hpf EBE 1 and 4 treatments either for PO or BW. These results are in agreement with the developmental stage-specific sensitivity highlighted by the three dose-response curves, confirming gastrulae as the most sensitive stage to the extract with the lowest EC_{50} (5.366 μg mL^{-1}) and plutei as the most resistant stage with an EC_{50} equal to 16.46 μg mL^{-1}, probably because of gastrulae incomplete development and suboptimal protective mechanisms, such as the induction of HSPs and autophagy (see below). Exposure to the highest concentration (EBE 40) caused a 100% inhibition of cleavage and inevitably lead to an apoptotic-driven cell death regardless the exposure starting time, with no possibility of recovery.

Several biomarkers were used to detect the activation of the cellular stress response to EBE in *A. lixula* embryos, showing that it strongly depended on the developmental exposure window. The first cellular stress response mechanisms activated were the induction of HSP 60 and autophagy, similarly to our previous results on the hierarchical cellular stress response of *P. lividus* embryos exposed to environmental stressors (Matranga et al., 2013; Chiarelli et al., 2016). Larvae exposed from the pluteus stage had a HSP 60 induction greater than larvae exposed from the gastrula stage, probably accounting for the better resistance of plutei. As seen from the LC3 and p62/SQSTM1 markers, autophagy was massively induced in both 24 and 48 hpf treatments, indicating the effort of gastrulae and plutei to remove toxic metabolites, misfolded/damaged proteins and organelles. On the contrary, in the 0 hpf treatments we found a time-dependent decrease of autophagy, in parallel with the induction of apoptosis as seen with two markers: cleaved

caspase-7, known to play a key role in the execution-phase of apoptosis, and CHOP-10/GADD153, whose overexpression is linked to cell cycle arrest leading to apoptosis. The *in situ* analysis of fragmented DNA showed that apoptosis was acting either as a selective process at low doses (EBE 4) affecting only some cells, likely the most damaged, or as a process involving the whole embryo at high doses (EBE 40), leading to death. This selective apoptosis is reasonably acting to preserve the developmental program since other cells may benefit from the materials liberated by apoptotic cells, e.g. amino acids and substrates for ATP (Somero, 2020), as was observed in *P. lividus* embryos exposed to vanadium and to the combined exposure of gadolinium and increased temperatures (Chiarelli et al., 2021; Martino et al., 2021).

To interpretate why this seaweed should produce natural toxins with a toxic effect on sea urchin embryos, we have to consider the ecological interactions between these two species, with the seaweed producing chemical substances against its grazers and the sea urchin embryos adopting molecular strategies to respond to these environmental natural toxins. Oxylipins are the probable agents of this reproductive failure in *A. lixula*, similarly to the stunting action generated by diatoms-derived oxylipins on *P. lividus* and copepods reproduction (Miralto et al., 1999; Varrella et al., 2014). As *A. lixula* normally grazes on *E. brachycarpa* present in its environment, the harmful effect on embryos but not on adults suggests that there may be greater vulnerability of the embryos, similarly to copepods that can be successfully cultivated from embryo to adult stage on diatom food (Koski et al., 1998). Extracts from different brown algae, including *Ericaria crinita*, showed larvicidal effects against the larvae of different insects (Fouda et al., 2022; Aly et al., 2023), suggesting their potential as natural resources for insecticides production. While the larvicidal effects of oxylipins were tested on *Drosophila* larvae, finding impairment of metamorphosis and toxic effects on pupae (Yin et al., 2015), plant extracts containing oxylipins were found to be toxic for the adult stages of different insects (Pavela et al., 2019), with promising insecticidal efficacy.

As previously mentioned, oxylipins have been shown to have toxic effects on several tumoral cell line, leading cancer cells to cell cycle arrest and/or apoptosis thanks to their triple bond making them highly alkylating molecules (Cohen and Flescher, 2009; Christensen, 2020), suggesting their potential therapeutic uses as anti-cancer drug. Our study showed that the treatment of neuroblastoma tumoral cells with the oxylipin-containing *E. brachycarpa* extract induced a dose-dependent reduction in cells viability, with 40 μg/mL killing 78% of the cells at 72 h, while no toxic effect was detected at this dose on the neuronal-like cells derivatives, demonstrating the EBE selectivity versus the proliferating phenotype. This selective effect of EBE on proliferating cells may be associated with a decrease of the HSPs, molecular chaperones involved in maintaining the structure of proteins under different stress conditions (Hu et al., 2022). Both HSP 60 and HSP 90 play a key role in tumorigenesis by regulating protein homeostasis in response to stress, and inhibitors of these chaperons are widely considered as cancer therapeutics (Park et al., 2020; Zhou et al., 2018). The strong and progressive reduction of both HSP 60 and HSP 90 in response to EBE treatment reveals a new mechanism underlying the potential anti-neoplastic activity of this extract of macroalgae containing oxylipins. Inhibition of HSP 60 and HSP 90, associated with the lack of HSP 70 expression in SH-SY5Y cells (Scordino et al., 2023) leads to the accumulation of unfolded or misfolded proteins in the endoplasmic reticulum, triggering the activation of a defense mechanism known as unfolded protein response, finally leading to apoptosis of SH-SY5Y cells (Read and Schröder, 2021). According to our results, EBE treatment produces a significant increase in CHOP/GADD153, a protein involved in ER stress-mediated apoptosis (Oyadomari and Mori, 2004), and the consequent increase of the cleaved form of Caspase-7. The activation of apoptosis was also confirmed by the increase in the percentage of fragmented DNA. Interestingly, we observed an increase in LC3 expression in response to 48 h EBE treatment, suggesting the induction of autophagy, a process that can be stimulated by several types of cellular stress, including ER stress. However, the role of autophagy induced by ER stress is controversial and likely dependent on the extent of ER stress (Rashid et al., 2015). Although most studies indicate that autophagy is a conserved cellular process that maintains cellular homeostasis, exerting pro-survival functions following ER stress, it has been also demonstrated that autophagy and apoptosis often occur in the same cell, mostly in a sequence in which autophagy precedes and facilitates apoptosis (Gump and Thorburn, 2011; Song et al., 2017). Here, the increase in the autophagic process in response to EBE treatment may indicate an attempt of proliferating cells to avoid being killed, or the effect of an intense ER stress which leads to autophagy-dependent cell apoptosis. Therefore, more research is needed to clarify the complex interplay between autophagy and apoptosis in EBE-exposed SH-SY5Y cells.

5. Conclusions

Our study is the first to test an oxylipin-containing macroalgae extract on invertebrate reproduction, giving new perspectives to elucidate the molecular strategies that marine invertebrates use when responding to their environmental natural toxins. Moreover, this is the first time that an oxylipins-containing extract from a macroalgae shows antineoplastic activity in a neuroblastoma cell line, showing the potential to selectively trigger apoptosis of cancer cells but not in the corresponding normal cells. Further studies are currently being carried out to fully characterize the chemical composition of EBE, to isolate each compound, to quantify the oxylipins' content and verify if it increases in stress conditions, such as in grazed algae. Once the effect of single molecules on embryo development and cancer cells will be well known, it will be possible to synthesize the molecules with the best anti-growth activities and further explore their potential as a prospective source for the development of innovative, environmentally friendly larvicides and antineoplastic compounds.

CRediT authorship contribution statement

Chiara Martino: Writing – original draft, Methodology, Investigation, Formal analysis, Conceptualization. **Rosario Badalamenti:** Visualization, Methodology, Investigation, Conceptualization. **Monica Frinchi:** Writing – original draft, Methodology, Investigation, Formal analysis, Conceptualization. **Roberto Chiarelli:** Visualization, Investigation. **Antonio Palumbo Piccionello:** Resources, Methodology. **Giulia Urone:** Investigation. **Manuela Mauro:** Resources, Methodology. **Vincenzo Arizza:** Project administration, Funding acquisition. **Claudio Luparello:** Writing – review & editing. **Valentina Di Liberto:** Writing – review & editing, Investigation. **Giuseppa Mudò:** Writing – review & editing. **Mirella Vazzana:** Writing – review & editing, Supervision, Funding acquisition, Conceptualization.

Declaration of competing interest

The authors declare that they have no known competing financial interests or personal relationships that could have appeared to influence the work reported in this paper.

Data availability

Data will be made available on request.

Acknowledgements

The authors would like to thank the National Biodiversity Future Center – NBFC, Project funded under the National Recovery and Resilience Plan (NRRP), Mission 4 Component 2 Investment 1.4 - Call for tender No. 3138 of December 16, 2021, rectified by Decree n.3175 of December 18, 2021 of Italian Ministry of University and Research

funded by the European Union – NextGenerationEU; Award Number: Project code CN_00000033, Concession Decree No. 1034 of June 17, 2022 adopted by the Italian Ministry of University and Research, CUP B73C22000790001, Project title "National Biodiversity Future Center - NBFC". PJ_UTILE_2022_VQR_Misura_B_D15_Palumbo from University of Palermo is gratefully acknowledged.

References

Adarshan, S., Sree, V.S.S., Muthuramalingam, P., Nambiar, K.S., Sevanan, M., Satish, L., Venkidasamy, B., Jeelani, P.G., Shin, H., 2023. Understanding macroalgae: a comprehensive exploration of nutraceutical, pharmaceutical, and omics dimensions. Plants 13. https://doi.org/10.3390/plants13010113.

Aly, S.H., Elissawy, A.M., Salah, D., Alfuhaid, N.A., Zyaan, O.H., Mohamed, H.I., Singab, A.N.B., Farag, S.M., 2023. Phytochemical investigation of three *cystoseira* species and their larvicidal activity supported with in silico studies. Mar. Drugs 21 (2), 117. https://doi.org/10.3390/md21020117.

Amico, V., 1995. Marine brown algae of family *Cystoseiraceae*: chemistry and chemotaxonomy. Phytochem. 39, 1257–1279.

Ávila-Román, J., Talero, E., de Los Reyes, C., Zubía, E., Motilva, V., García-Mauriño, S., 2016. Cytotoxic activity of microalgal-derived oxylipins against human cancer cell lines and their impact on ATP levels. Nat. Prod. Commun. 11, 1871–1875. https://doi.org/10.1177/1934578X1601101225.

Barbosa, M., Valentão, P., Andrade, P.B., 2016. Biologically active oxylipins from enzymatic and nonenzymatic routes in macroalgae. Mar. Drugs 14, 23. https://doi.org/10.3390/md14010023.

Blasio, M., Balzano, S., 2021. Fatty acids derivatives from eukaryotic microalgae, pathways and potential applications. Front. Microbiol. 12, 718933 https://doi.org/10.3389/fmicb.2021.718933.

Bonaviri, C., Vega Fernández, T., Fanelli, G., Badalamenti, F., Gianguzza, P., 2011. Leading role of the sea urchin *Arbacia lixula* in maintaining the barren state in southwestern Mediterranean. Mar. Biol. 158, 2505–2513. https://doi.org/10.1007/s00227-011-1751-2.

Budzałek, G., Śliwińska-Wilczewska, S., Wiśniewska, K., Wochna, A., Bubak, I., Latała, A., Wiktor, J.M., 2021. Macroalgal defense against competitors and herbivores. Int. J. Mol. Sci. 22 https://doi.org/10.3390/ijms22157865.

Byrne, M., Lamare, M., Winter, D., Dworjanyn, S.A., Uthicke, S., 2013. The stunting effect of a high CO_2 ocean on calcification and development in sea urchin larvae, a synthesis from the tropics to the poles. Philos. Trans. R. Soc. Lond. B Biol. Sci. 368, 20120439 https://doi.org/10.1098/rstb.2012.0439.

Chiarelli, R., Martino, C., Agnello, M., Bosco, L., Roccheri, M.C., 2016. Autophagy as a defense strategy against stress: focus on *Paracentrotus lividus* sea urchin embryos exposed to cadmium. Cell Stress Chaper. 21, 19–27. https://doi.org/10.1007/s12192-015-0639-3.

Chiarelli, R., Martino, C., Roccheri, M.C., Cancemi, P., 2021. Toxic effects induced by vanadium on sea urchin embryos. Chemosphere 274, 129843. https://doi.org/10.1016/j.chemosphere.2021.129843.

Christensen, L.P., 2020. Bioactive C17 and C18 acetylenic oxylipins from terrestrial plants as potential lead compounds for anticancer drug development. Molecules 25 (11), 2568. https://doi.org/10.3390/molecules25112568.

Cohen, S., Flescher, E., 2009. Methyl jasmonate: a plant stress hormone as an anti-cancer drug. Phytochem 70, 1600–1609. https://doi.org/10.1016/j.phytochem.2009.06.007.

Conte, M., Fontana, E., Nebbioso, A., Altucci, L., 2020. Marine-derived secondary metabolites as promising epigenetic bio-compounds for anticancer therapy. Mar. Drugs 19. https://doi.org/10.3390/md19010015.

de Sousa, Gangadhar, K.N., Macridachis, J., Pavao, M., Morais, T.R., Campino, L., Valera, J., Lago, J.H.G., 2017. *Cystoseira* algae (Fucaceae): Update on their chemical entities and biological activities. Tetrahedron: Asymmetry 28 (11), 1486–1505. https://doi.org/10.1016/j.tetasy.2017.10.014.

Dhamdhere, M.R., Spiegelman, V.S., 2024. Extracellular vesicles in neuroblastoma: role in progression, resistance to therapy and diagnostics. Front. Immunol. 9 (15), 1385875 https://doi.org/10.3389/fimmu.2024.1385875.

Faddetta, T., Polito, G., Abbate, L., Alibrandi, P., Zerbo, M., Caldiero, C., Reina, C., Puccio, G., Vaccaro, E., Abenavoli, M.R., Cavalieri, V., Mercati, F., Palumbo Piccionello, A., Gallo, G., 2023. Bioactive metabolite survey of actinobacteria showing plant growth promoting traits to develop novel biofertilizers. Metabolites 13. https://doi.org/10.3390/metabo13030374.

Fontana, A., d'Ippolito, G., Cutignano, A., Miralto, A., Ianora, A., Romano, G., Cimino, G., 2007. Chemistry of oxylipin pathways in marine diatoms. Pure Appl. Chem. 79 (4), 481–490. https://doi.org/10.1351/pac200779040481.

Fouda, A., Eid, A.M., Abdel-Rahman, M.A., El-Belely, E.F., Awad, M.A., Hassan, S.E., Al-Faifi, Z.E., Hamza, M.F., 2022. Enhanced antimicrobial, cytotoxicity, larvicidal, and repellence activities of Brown algae. Front. Bioeng. Biotechnol. 10, 849921 https://doi.org/10.3389/fbioe.2022.849921.

Gerwick, W.H., Singh, I.P., 2002. Structural diversity of marine oxylipins. In: Gardner, H. W., Kuo, T.M. (Eds.), Lipid Biotechnology. Marcel and Dekker, New York, pp. 249–275.

Gomes, M.P., Garcia, Q.S., Barreto, L.C., Pimenta, L.P.S., Matheus, M.T., Figueredo, C.C., 2017. Allelopathy: an overview from micro-to macroscopic organisms, from cells to environments, and the perspectives in a climate-changing world. Biologia 72, 113–129. https://doi.org/10.1515/biolog-2017-0019.

Gump, J.M., Thorburn, A., 2011. Autophagy and apoptosis: what is the connection? Trends Cell Biol. 21, 387–392. https://doi.org/10.1016/j.tcb.2011.03.007.

Hoffmann, L., Renard, R., Demoulin, V., 1992. Phenology, growth and biomass of *Cystoseira balearica* in Calvi (Corsica). Mar. Ecol.: Prog. Ser. 80, 249–254.

Hu, C., Yang, J., Qi, Z., Wu, H., Wang, B., Zou, F., Mei, H., Liu, J., Wang, W., Liu, Q., 2022. Heat shock proteins: biological functions, pathological roles, and therapeutic opportunities. Media Commun. 3, e161. https://doi.org/10.1002/mco2.161.

Jacquemoud, D., Pohnert, G., 2015. Extraction and analysis of oxylipins from macroalgae Illustrated on the example *Gracilaria vermiculophylla*. Methods Mol. Biol. 1308, 159–172.

Koski, M., Klein, B.W., Schogt, N., 1998. Effect of food quality on rate of growth and development of the pelagic copepod *Pseudocalanus elongatus* (Copepoda, Calanoida). Mar. Ecol. Prog. Ser. 170, 169–187. https://doi.org/10.3354/meps170169.

Lauritano, C., Ianora, A., 2020. Chemical defense in marine organisms. Mar. Drugs 18 (10), 518. https://doi.org/10.3390/md18100518.

Lawrence, J.M., 2013. Sea Urchins: Biology and Ecology, third ed. Elsevier, London.

Librizzi, M., Martino, C., Mauro, M., Abruscato, G., Arizza, V., Vazzana, M., Luparello, C., 2023. Natural anticancer peptides from marine animal species: evidence from in vitro cell model systems. Cancers 16. https://doi.org/10.3390/md18100518.

Luo, X., Li, F., Hong, J., Lee, C.O., Sim, C.J., Im, K.S., Jung, J.H., 2006. Cytotoxic oxylipins from a marine sponge *Topsentia* sp. J. Nat. Prod. 69, 567–571. https://doi.org/10.1021/np0503552.

Martino, C., Byrne, M., Roccheri, M.C., Chiarelli, R., 2021. Interactive effects of increased temperature and gadolinium pollution in *Paracentrotus lividus* sea urchin embryos: a climate change perspective. Aquat. Toxicol. 232, 105750 https://doi.org/10.1016/j.aquatox.2021.105750.

Matranga, V., Pinsino, A., Bonaventura, R., Costa, C., Karakostis, K., Martino, C., Russo, R., Zito, F., 2013. Cellular and molecular bases of biomineralization in sea urchin embryos. Cah. Biol. Mar. 54, 467–478.

Miralto, A., Barone, G., Romano, G., Poulet, S.A., Ianora, A., Russo, G.L., Buttino, I., Mazzarella, G., Laabir, M., Giacobbe, M.G., 1999. The insidious effect of diatoms on copepod reproduction. Nature 402 (6758), 173–176.

Molinari-Novoa, E.A., Guiry, M.D., 2020. Reinstatement of the genera *Gongolaria* Boehmer and *Ericaria* Stackhouse (Sargassaceae, Phaeophyceae). Notulae Algarum 171, 1–10.

Nuzzo, D., Frinchi, M., Giardina, C., Scordino, M., Zuccarini, M., De Simone, C., Di Carlo, M., Belluardo, N., Mudò, G., Di Liberto, V., 2023. Neuroprotective and antioxidant role of oxotremorine-M, a non-selective muscarinic acetylcholine receptors agonist, in a cellular model of Alzheimer disease. Cell. Mol. Neurobiol. 43, 1941–1956. https://doi.org/10.1007/s10571-022-01274-9.

Nuzzo, D., Picone, P., Giardina, C., Scordino, M., Mudò, G., Pagliaro, M., Scurria, A., Meneguzzo, F., Ilharco, L.M., Fidalgo, A., Alduina, R., Presentato, A., Ciriminna, R., Di Liberto, V., 2021. New neuroprotective effect of lemon IntegroPectin on neuronal cellular model. Antioxidants 10. https://doi.org/10.3390/antiox10050669.

Oyadomari, S., Mori, M., 2004. Roles of CHOP/GADD153 in endoplasmic reticulum stress. Cell Death Differ. 11, 381–389. https://doi.org/10.1038/sj.cdd.4401373.

Park, H.K., Yoon, N.G., Lee, J.E., Hu, S., Yoon, S., Kim, S.Y., Hong, J.H., Nam, D., Chae, Y.C., Park, J.B., Kang, B.H., 2020. Unleashing the full potential of Hsp90 inhibitors as cancer therapeutics through simultaneous inactivation of Hsp90, Grp94, and TRAP1. Exp. Mol. Med. 52, 79–91. https://doi.org/10.1038/s12276-019-0360-x.

Pavela, R., Maggi, F., Cianfaglione, K., Canale, A., Benelli, G., 2019. Promising insecticidal efficacy of the essential oils from the halophyte *Echinophora spinosa* (Apiaceae) growing in Corsica Island, France. Environ. Sci. Pollut. Res. 27, 14454–14464. https://doi.org/10.1007/s11356-019-04980-y.

Pereira, L., Cotas, J., 2023. Therapeutic potential of polyphenols and other micronutrients of marine origin. Mar. Drugs 21. https://doi.org/10.3390/md21060323.

Privitera, D., Chiantore, M., Mangialajo, L., Glavic, N., Kozul, W., Cattaneo-Vietti, R., 2008. Inter-and intra-specific competition between *Paracentrotus lividus* and *Arbacia lixula* in resource-limited barren areas. J. Sea Res. 60 (3), 184–192. https://doi.org/10.1016/j.seares.2008.07.001.

Rashid, H.O., Yadav, R.K., Kim, H.R., Chae, H.J., 2015. ER stress: autophagy induction, inhibition and selection. Autophagy 11, 1956–1977. https://doi.org/10.1080/15548627.2015.1091141.

Read, A., Schröder, M., 2021. The unfolded protein response: an overview. Biology 10. https://doi.org/10.3390/biology10050384.

Ritter, A., Goulitquer, S., Salaün, J.P., Tonon, T., Correa, J.A., Potin, P., 2008. Copper stress induces biosynthesis of octadecanoid and eicosanoid oxygenated derivatives in the brown algal kelp *Laminaria digitata*. New Phytol. 180 (4), 809–821. https://doi.org/10.1111/j.1469-8137.2008.02626.x.

Romano, G., Miralto, A., Ianora, A., 2010. Teratogenic effects of diatom metabolites on sea urchin *Paracentrotus lividus* embryos. Mar. Drugs 8, 950–967. https://doi.org/10.3390/md8040950.

Ruocco, N., Annunziata, C., Ianora, A., Libralato, G., Manfra, L., Costantini, S., Costantini, M., 2019. Toxicity of diatom-derived polyunsaturated aldehyde mixtures on sea urchin *Paracentrotus lividus* development. Sci. Rep. 9, 517. https://doi.org/10.1038/s41598-018-37546-y.

Sansone, C., Braca, A., Ercolesi, E., Romano, G., Palumbo, A., Casotti, R., Francone, M., Ianora, A., 2014. Diatom-derived polyunsaturated aldehydes activate cell death in human cancer cell lines but not normal cells. PLoS One 9 (7), e101220. https://doi.org/10.1371/journal.pone.0101220.

Savchenko, T., Degtyaryov, E., Radzyukevich, Y., Buryak, V., 2022. Therapeutic potential of plant oxylipins. Int. J. Mol. Sci. 23 https://doi.org/10.3390/ijms232314627.

Scordino, M., Frinchi, M., Urone, G., Nuzzo, D., Mudò, G., Di Liberto, V., 2023. Manipulation of HSP70-SOD1 expression modulates SH-SY5Y differentiation and susceptibility to oxidative stress-dependent cell damage: involvement in oxotremorine-M-mediated neuroprotective effects. Antioxidants 12. https://doi.org/10.3390/antiox12030687.

Scordino, M., Urone, G., Frinchi, M., Valenza, C., Bonura, A., Cipollina, C., Ciriminna, R., Meneguzzo, F., Pagliaro, M., Mudò, G., Di Liberto, V., 2024. Anti-apoptotic and anti-inflammatory properties of grapefruit IntegroPectin on human microglial HMC3 cell line. Cells 13. https://doi.org/10.3390/cells13040355.

Seth, T., Asija, S., Umar, S., Gupta, R., 2024. The intricate role of lipids in orchestrating plant defense responses. Plant Sci. 338, 111904 https://doi.org/10.1016/j.plantsci.2023.111904.

Somero, G.N., 2020. The cellular stress response and temperature: function, regulation, and evolution. J. Exp. Zool. A Ecol. Integr. Physiol. 333, 379–397. https://doi.org/10.1002/jez.2344.

Song, S., Tan, J., Miao, Y., Li, M., Zhang, Q., 2017. Crosstalk of autophagy and apoptosis: involvement of the dual role of autophagy under ER stress. J. Cell. Physiol. 232, 2977–2984. https://doi.org/10.1002/jcp.25785.

Thaman, J., Pal, R.S., Chaitanya, M.V.N.L., Yanadaiah, P., Thangavelu, P., Sharma, S., Amoateng, P., Arora, S., Sivasankaran, P., Pandey, P., Mazumder, A., 2023. Reconciling the gap between medications and their potential leads: the role of marine metabolites in the discovery of new anticancer drugs: a comprehensive review. Curr. Pharmaceut. Des. 29 (39), 3137–3153. https://doi.org/10.2174/0113816128272025231106071447.

Varrella, S., Romano, G., Ianora, A., Bentley, M.G., Ruocco, N., Costantini, M., 2014. Molecular response to toxic diatom-derived aldehydes in the sea urchin *Paracentrotus lividus*. Mar. Drugs 12 (4), 2089–2113. https://doi.org/10.3390/md12042089.

Varrella, S., Romano, G., Ruocco, N., Ianora, A., Bentley, M.G., Costantini, M., 2016. First morphological and molecular evidence of the negative impact of diatom-derived hydroxyacids on the sea urchin *Paracentrotus lividus*. Toxicol. Sci. 151 (2), 419–433. https://doi.org/10.1093/toxsci/kfw053.

Wangensteen, O.S., Turon, X., Casso, M., Palacín, C., 2013. The reproductive cycle of the sea urchin *Arbacia lixula* in northwest Mediterranean: potential influence of temperature and photoperiod. Mar. Biol. 160, 3157–3168. https://doi.org/10.1007/s00227-013-2303-8.

Yin, G., Padhi, S., Lee, S., Hung, R., Zhao, G., Bennett, J.W., 2015. Effects of three volatile oxylipins on colony development in two species of fungi and on *Drosophila* larval metamorphosis. Curr. Microbiol. 71 (3), 347–356. https://doi.org/10.1007/s00284-015-0864-0.

Zhou, C., Sun, H., Zheng, C., Gao, J., Fu, Q., Hu, N., Shao, X., Zhou, Y., Xiong, J., Nie, K., Zhou, H., Shen, L., Fang, H., Lyu, J., 2018. Oncogenic HSP 60 regulates mitochondrial oxidative phosphorylation to support Erk1/2 activation during pancreatic cancer cell growth. Cell Death Dis. 9 (2), 161. https://doi.org/10.1038/s41419-017-0196-z.